Chin. J. Astron. Astrophys. Vol. 3 (2003), No. 5, 395–409
(*http://www.chjaa.org* or *http://chjaa.bao.ac.cn*)

Chinese Journal of Astronomy and Astrophysics

Time Scales and Tidal Effects in Minor Mergers

Yu Lu and Jian-Yan Wei

National Astronomical Observatories, Chinese Academy of Sciences, Beijing 100012;
luyu@nova.astro.umass.edu

Received 2003 February 27; accepted 2003 June 18

Abstract We use controlled N-body simulation to investigate the dynamical processes (dynamical friction, tidal truncation, etc.) involved in the merging of small satellites into bigger halos. We confirm the validity of some analytic formulae proposed earlier based on simple arguments. For rigid satellites represented by softened point masses, the merging time scale depends on both the orbital shape and concentration of the satellite. The dependence on orbital ellipticity is roughly a power law, as suggested by Lacey & Cole, and the dependence on satellite concentration is similar to that proposed by White. When merging satellites are represented by non-rigid objects, Tidal effects must be considered. We found that material beyond the tidal radius are stripped off. The decrease in the satellite mass might mean an increase in the merging time scale, but in fact, the merging time is decreased, because the stripped-off material carries away a proportionately larger amount of of orbital energy and angular momentum.

Key words: cosmology: dark matter — galaxies: kinematics and dynamics — galaxies: structure — galaxies: interactions — numerical methods

1 INTRODUCTION

Minor mergers, in which a small object (the satellite) merges into a large one (the host), is an important phenomenon in galaxy formation and evolution. In the hierarchical cosmogony such as the cold dark matter (CDM) model, where the build-up of cosmic structure proceeds from small to large scales, mergers of small dark matter halos and galaxies into larger systems are expected to be common.

There are two key dynamical processes involved in such minor mergers. One is dynamical friction, which is the resistance force experienced by a merging satellite as it goes through the medium of mass particles, and the other is tidal stripping, by which the material in the outer part of the satellite is stripped off due to tidal force of the host. Simple analytic models have been proposed to describe these processes. For the dynamical friction, a widely adopted model is the Chandrasekkar's dynamical friction formula (Chandrasekkar 1943). This formula

∗ Supported by the National Natural Science Foundation of China.

was derived under the assumptions that the satellite is a point mass and that the host is a uniform distribution of mass particles. Although subsequent numerical simulations show that Chandrasekkar's formula may be a good approximation in cases where the assumptions made in the derivation are valid (e.g. Bontekoe & van Albada 1987), it still remains unclear how accurate the formula is for realistic systems where the satellite is extended and can be stripped by tidal force, and where the host may have a significant density gradient. Indeed, as discussed in White (1976), the concentration of the satellite can affect the dynamic friction significantly. Tidal stripping is usually modelled with the tidal approximation. Although the tidal radius predicted by the tidal approximation may be used to characterize the place where mass stripping becomes significant, tidal heating may cause the satellite to expand, thus the tidal truncation is not sharp at the tidal radius (Hayashi et al. 2002). Furthermore, tidal stripping can also affect the dynamic friction exerted on the satellite.

Ideally, we should use cosmological simulations to study minor mergers in cosmic structure formation where the orbits of the mergers and the structures of both the host and satellite are modeled realistically. Unfortunately, because of the limited numerical resolutions, satellites can only be sampled by a small number of particles, and so it is difficult to model the relevant processes accurately. In addition, in a cosmological simulation different processes may work simultaneously and it is difficult to figure out the importance of the individual processes.

In this paper, we carry out a series of controlled simulations of minor mergers to investigate how dynamical friction and tidal stripping affect the merger of satellites into host halos. The simulations are designed to cover a relatively large range in orbital configuration, in the mass ratio between satellite and host and in the concentration of the satellite. Satellites are either assumed to be rigid, thus the tidal effect is irrelevant, or are represented by a large number of particles when studying the effects due to tidal stripping. The outline of this paper is as follows. In Section 2 we present our halo model and describe the simulations. In Section 3 we show the results for rigid satellites to demonstrate how the merging time depends on the concentration of the satellite. Results for non-rigid satellites are given in Section 4 to demonstrate how tidal stripping affects the merger time scale, and we also discuss how tidal interaction affects the structure of the satellite. Our main conclusions and a further discussion are given in Section 5.

2 NUMERICAL EXPERIMENTS

We use GADGET, an N-body code developed by Springel, to perform the simulations. Details about this code and its performance can be found in Springel et al. (2001). The code is an N-body/SPH-code in C, specifically designed for the simulation of galaxy formation and interaction. The gravitational interaction is either computed with a Tree algorithm or with the special-purpose hardware GRAPE. In the present work, the SPH part of GADGET is not used, and we just treat the halo material as collisionless particles. The Parallel version of GADGET-1.1 is employed in these simulations.

We consider two models for the initial host halos. In one model, the halo profile is a truncated isothermal sphere as described in Binney & Tremaine (1987):

$$\rho_{\rm sis}(r) = \frac{{V_{\rm c}}^2}{4\pi G r^2}, \tag{1}$$

where $V_{\rm c}$ is the circular velocity, and the profile is truncated at a radius $R = 50\,{\rm kpc}$ so that $V_{\rm c}$ is related to the mass of the halo by $V_{\rm c}^2 = GM/R$. The other model assumes a Hernquist

profile (1990),

$$\rho_{\rm h}(r) = \frac{M}{2\pi}\frac{a}{r(r+a)^3}, \tag{2}$$

where M is the total mass of the halo and a is a scale parameter, related to the half-mass radius (within which half of the halo mass is contained) by $a = R_{\rm h}(\sqrt{2}-1)$. A comparison between the two halo types probes the effect of halo profile. Note that the Hernquist profile can be used to approximate a CDM halo with the Navarro, Frenk & White (1996) profile in the inner region, as shown in Fig. 1. All host halos are constructed using the distribution functions assuming isotropic velocity dispersion. We evolve each halo over about 20 dynamical times to ensure that the prepared halo is stable. In most of our simulations we used 10^4 particles to represent the host halo; for one typical case we used 10^5 particles to test the reliability of our results.

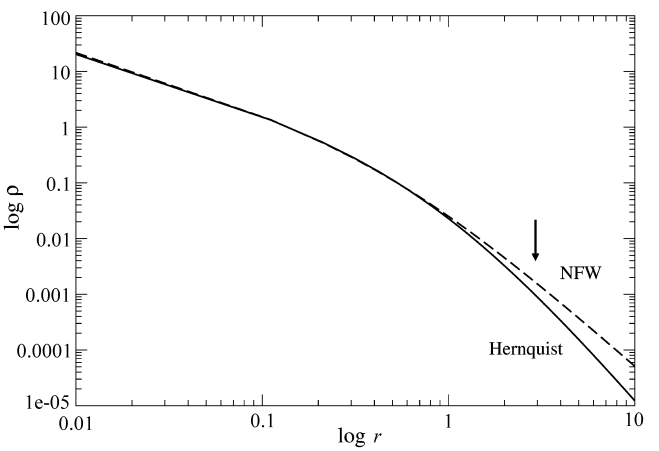

Fig. 1 Similarity of the density profile of the Hernquist model and the NFW model. The solid line is the density profile of the Hernquist model used to model the host halo in Model D series, and the dashed line is for a NFW halo. The mass distributions of the two are quite similar in the inner region. The arrow points at the initial radius of the satellites at the beginning of our simulations. It is reasonable to use the Hernquist model to mimic the NFW in the merging experiments of this paper.

The satellites are represented either by a softened point mass or a Hernquist profile sampled by 10^4 particles. In the former case, the satellite is rigid with density profile represented by the spline function and so cannot be stripped. In the latter case all the dynamical processes are allowed in the N-body system. We vary the scale radius of the softening ϵ or the half-mass radius $R_{\rm h}$ to change the concentration of the satellite in these two cases.

We carried out several sets of simulation differing in the host and satellite properties, in the satellite/host mass ratio $M_{\rm s}/M_{\rm h}$, and in orbital configurations. The orbital configuration is specified by the ratio $\varepsilon \equiv J/J_{\rm C}(E)$, where J is the angular momenmtum of the satellite and $J_{\rm C}(E)$ is that of the circular orbit with the same energy E as the satellite (Lacey & Cole 1993; Velázquez & White 1999). The parameters for all the simulated host/satellite systems are summarized in Table 1. In all the presentations, mass is in units of $10^{11}M_{\odot}$, time is in 10^8

years, and length is in 10 kpc. In all of our simulations, the masses of the host halos ($M_{\rm h}$) are fixed at 2.

The softening length of the host particles is 0.0136 and that of satellite particles is 0.0063. These softening lengths are set large enough to avoid two-body relaxation. This is also consistent with van Kampen (2000) who suggested that $\varepsilon = 0.77 r_{\rm h} N^{-1/3}$, where $r_{\rm h}$ is the half mass radius of the halo and N is the total number of particles. The time steps are set small enough for the energy to be conserved to an accuracy of $\frac{\triangle E_{\rm tot}}{E_{\rm tot}} < 1\%$.

Table 1 Parameters of Numerical Merging Experiments

	Host halos			Satellites				
run	N_p	density profile	$R_{\rm h}$	N_p	density profile	$R_{\rm h}/\epsilon$	ε	$M_{\rm s}/M_{\rm h}$
A1	10^4	singular isothermal sphere	$\cdots$	1	spline	0.2	1.00	0.1
A2	10^4	singular isothermal sphere	$\cdots$	1	spline	0.2	0.82	0.1
A3	10^4	singular isothermal sphere	$\cdots$	1	spline	0.2	0.55	0.1
A4	10^4	singular isothermal sphere	$\cdots$	1	spline	0.2	0.33	0.1
B1	10^4	Hernquist	0.38	1	spline	0.2	1.00	0.1
B2	10^4	Hernquist	0.38	1	spline	0.2	0.82	0.1
B3	10^4	Hernquist	0.38	1	spline	0.2	0.55	0.1
B4	10^4	Hernquist	0.38	1	spline	0.2	0.33	0.1
B5	10^4	Hernquist	0.38	1	spline	0.1	1.00	0.1
B6	10^4	Hernquist	0.38	1	spline	0.05	1.00	0.1
C1	10^4	Hernquist	0.38	10^4	Hernquist	0.18	1.00	0.1
C2	10^4	Hernquist	0.38	10^4	Hernquist	0.18	0.82	0.1
C3	10^4	Hernquist	0.38	10^4	Hernquist	0.18	0.55	0.1
C4	10^4	Hernquist	0.38	10^4	Hernquist	0.18	0.33	0.1
D1	10^4	Hernquist	2.20	10^4	Hernquist	1.0	1.00	0.1
D2	10^4	Hernquist	2.20	10^4	Hernquist	1.0	0.82	0.1
D3	10^4	Hernquist	2.20	10^4	Hernquist	1.0	0.55	0.1
D4	10^4	Hernquist	2.20	10^4	Hernquist	1.0	0.33	0.1
E1	10^4	Hernquist	0.38	10^4	Hernquist	0.22	1.00	0.2
E2	10^4	Hernquist	0.38	10^4	Hernquist	0.26	1.00	0.33
F1	10^5	Hernquist	0.38	10^5	Hernquist	0.18	1.00	0.1

Note: N_p denotes particle number of the halo, ϵ is the length scale for rigid satellites, 2.8ϵ equals the radius of the spline sphere. $R_{\rm h}$ is the half-mass radius for the Hernquist model, ε denotes the 'circularity' of the satellite orbit, which has been defined as $\varepsilon \equiv J/J_{\rm C}(E)$, where J is the angular momentum of the satellites and $J_{\rm C}(E)$ is that of a circular orbit of the same energy E (Lacey & Cole 1993; Velázquez & White 1999). $M_{\rm s}/M_{\rm h}$ is the mass ratio of the satellite to the host.

3 MERGING TIME FOR RIGID SATELLITES

Models in series A and B all have satellites modeled by a softened point mass. These two series differ in the assumption about the density profile of the host halos: Modal A assumes a singular isothermal sphere while B assumes a Hernquist profile. These two series are designed to show how dynamical friction depends on the density profile of the host, on the concentration of the satellite and on orbital configuration.

We study the orbital decay of the satellite due to dynamical friction by analyzing the evolution of the orbital radius, defined as the distance between the center of the host and that of the satellite. The evolutions of the orbits are shown in Fig. 2. We define the merging time

to be the time when the orbital radius has shrunk to 0.1 of its initial value (i.e. 1 kpc).

According to Chandrasekhar (1943), the dynamical friction is

$$\boldsymbol{F}_{\rm df} = -4\pi G^2 \ln\Lambda M_s^2 B(v/\sqrt{2}\sigma)\frac{\boldsymbol{v}}{v^3}, \tag{3}$$

where $\boldsymbol{v}$ is the satellite velocity, and the function $B(\chi)$ is defined as

$$B(\chi) \equiv {\rm erf}(\chi) - \frac{2\chi}{\sqrt{\pi}}e^{-\chi^2}, \tag{4}$$

where $\ln\Lambda \approx \ln(rv^2/GM_{\rm s})$ is the Coulomb logarithm (see Binney & Tremaine 1987, section 7.1). From this, one can calculate the merging time $\tau_{\rm merg}$. Obviously, the merging time scale will depend on the orbital circularity ε. Lacey & Cole (1993) argued for a power-law dependence, $\tau_{\rm merg} \propto \varepsilon^{\alpha}$ with $\alpha \sim 0.78$ for a satellite orbiting in a singular isothermal sphere. Figure 3 shows our results of the $\tau_{\rm merg}$-ε relations for models in A and B series. Fitting the relations by a power law, we obtain $\alpha = 0.89$ for series A, consistent with the results of Lacey & Cole (1993). The power index we obtained for model B is slightly larger, $\alpha \sim 1.24$.

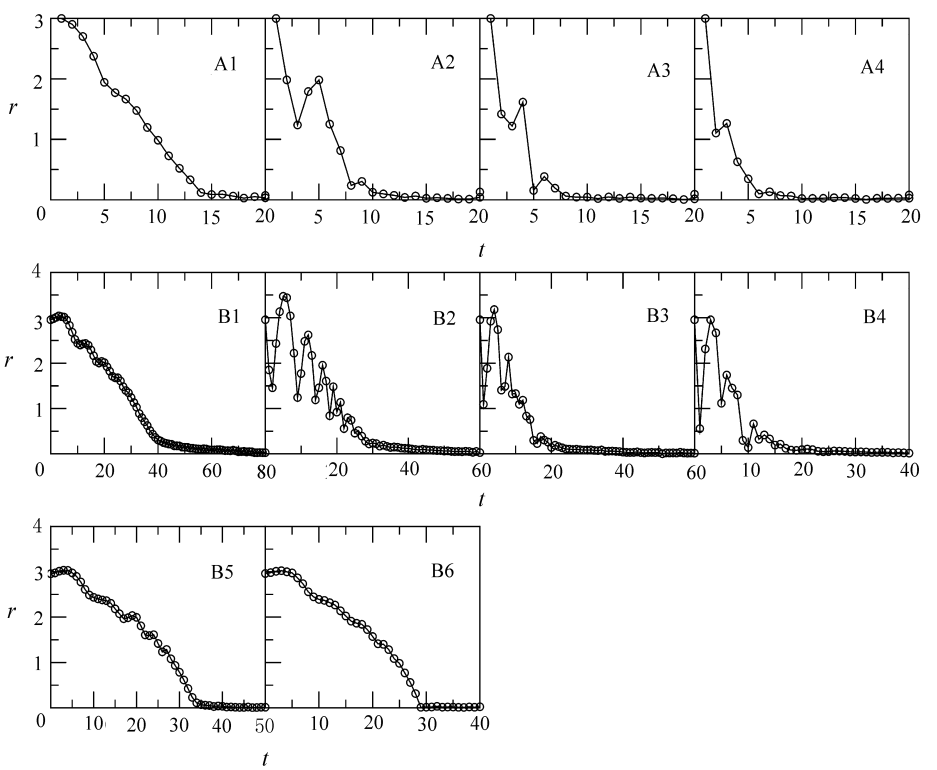

Fig. 2 Orbital decay of rigid satellites. The X-axes of these panels are time in units of 10^8 years. The Y-axes are the orbital radii of simulated satellites in units of 10 kpc, The solid lines with circles show the orbit evolution. The name of the model is shown in the upper right corner of each frame. In these models the satellites are modeled by rigid spline spheres. No tidal effects are included in these simulations, so the orbit decay is only due to dynamical friction.

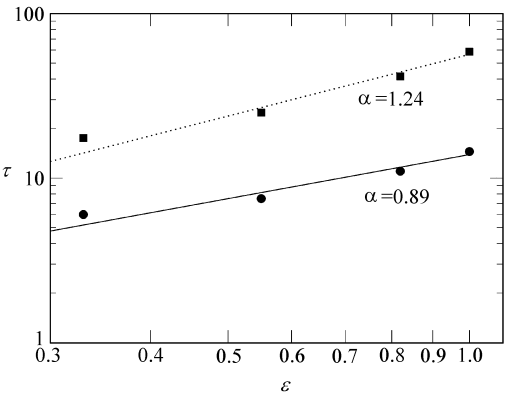

Fig. 3 Relation between the merging time scale and the orbital circularity of satellites. Circular dots are for model A1–A4, and squares for model B1–B4. The solid and dotted lines are the best fit lines for the data points. The merging time scale has a power-law dependence on the circularity, $\tau \propto \varepsilon^{\alpha}$, and the best fit α is indicated on the figure. The power index differs according to the mass distribution of the host.

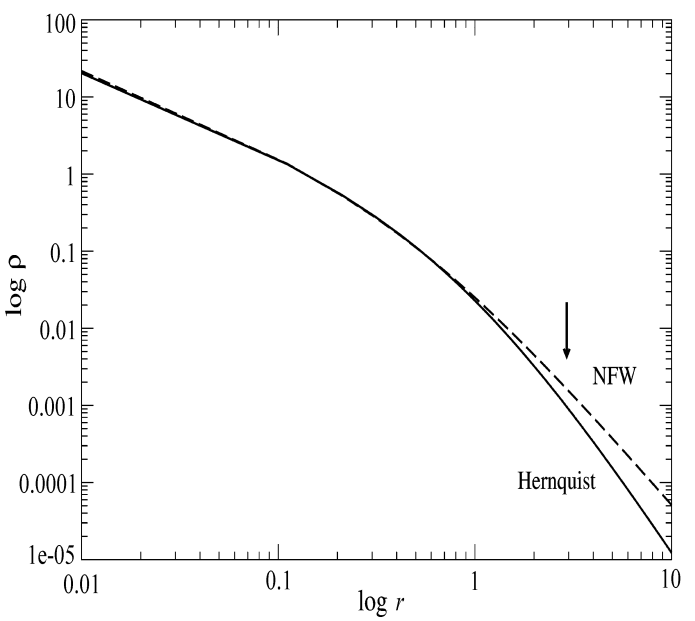

Fig. 4 In these panels $\ln \Lambda$ is calculated with Equation 6 for satellites in Model B1, B5 and B6, ϵ is softening of the satellite particle. Note the radius of the spline sphere $h = 2.8\epsilon$, and τ is the merging time of the investigated satellite observed in the simulations.

In the original derivation of the dynamical friction formula, Chandrasekhar assumed the satellite to be a point mass. This assumption may not hold for applications where the satellites are extended. This limitation of the original Chandrasekhar's formula was discussed by White (1976), who suggested that the Coulomb logarithm for extended satellites should be replaced by

$$\ln \Lambda = \frac{1}{M_{\rm sat}^2} \int_0^{d_{\rm max}} D^3 \Big[\int_D^\infty \frac{M_{\rm sat}(r) dr}{r^2 (r^2 - D^2)^{1/2}} \Big]^2 dD, \tag{5}$$

where $M_{\rm sat}(r)$ is the mass profile and $M_{\rm sat}$ is the total mass of the satellite. The upper limit of the integration $d_{\rm max}$ is the maximum impact parameter, which is set to be the half mass radius of the host. To test the validity of White's formula, we consider models in series B, where the satellites are represented by softened particles with different sizes (see Table 1). In GADGET, the density profile of each particle is the spline function (Springel et al. 2001), and so we also regard this function as the profiles of our softened satellites.

The upper left panel of Fig. 4 shows the simulation results of merging time for satellites with different extensions. For comparison, we use Eq. (5) to calculate the corresponding Coulomb logarithms in Model B1, B5 and B6. Since the merging time scale should be proportional to $1/\ln\Lambda$, the fact that the simulated merging time increases with the calculated $1/\ln\Lambda$ almost linearly (see the lowest panel of Fig. 4) implies that White's formula is valid.

4 RESULTS FOR NON-RIGID SATELLITES

In order to understand minor mergers in more realistic cases, we have carried out simulations with non-rigid satellites. In these models the satellite is modeled by the Hernquist halo with 10^4 particles. We now investigate the merging time and its dependence on tidal effects.

In tidal interaction some part of the satellite mass may be stripped off during the merging. In order to study this we must identify the particles that are stripped off. We calculate the binding energy of each satellite particle in the potential well of the satellite and identify those with positive energies to be ones that have escaped from the satellite. Note that the binding energy is calculated using only particles that are still bound to the satellite. We iterate the procedure eight times to obtain stable membership (Sensui et al. 2002; Tormen et al. 1998). Figure 5 shows the time evolution of the orbit and mass of the satellite.

When tidal stripping is included in the merging process, the merging time scale is affected. In Fig. 6 we show the relation between the merging time and orbital circularity for the series C models. We see that the relation can still be fitted with a power-law, and the power index is about 1.7. The slope is different from what we obtained for rigid satellites. From Equation (3), one may think that tidal stripping should prolong the merging time scale, because it reduces the mass of the satellite and dynamical friction is proportional to the mass squared. This expectation would be correct, if the Coulomb logarithm remain to be the same and no other processes consume the orbital angular momentum of the satellite. When using Eq. (5) to calculate the Coulomb logarithms for the C series models, we indeed find that $\ln\Lambda$ is not larger than that in Models B1-B4. However, our simulations show an opposite result in the sense that the merging time is shortened (instead of prolonged) in the presence of tidal stripping. This interesting result is confirmed by simulation F1, whose resolution is 10 times higher than that of C series. Except the particle number, all other configurations of F1 are the same as that of C1. The orbital decay of C1 and F1 are compared in Fig. 7. The shortening of the merging

time scale of non-rigid satellites may be due to two causes. One is that with mass at the outer part stripped, the structure of the satellite becomes more concentrated, which has the effect of increasing the Coulomb logarithm. The other is that the stripped material has preferentially high orbital angular momentum, which accelerates the decay of the satellite orbit. In order to identify that the two effects are responsible for the effect we observed, we apply White's formula (equation (5)) to calculate $\ln\Lambda$ at each time step using the mass distribution of the satellite at the time. As expected, $\ln\Lambda$ increases with time (see Fig. 8) because tidal stripping makes the satellite more and more concentrated. However, the product of $m_{\rm sat}(t)$ and $\ln\Lambda$, which gives the dynamical friction in Chandrasekhar's dynamical friction formula, has no obvious trend in time. Thus, the change of merging time scale cannot be due to tidal truncation.

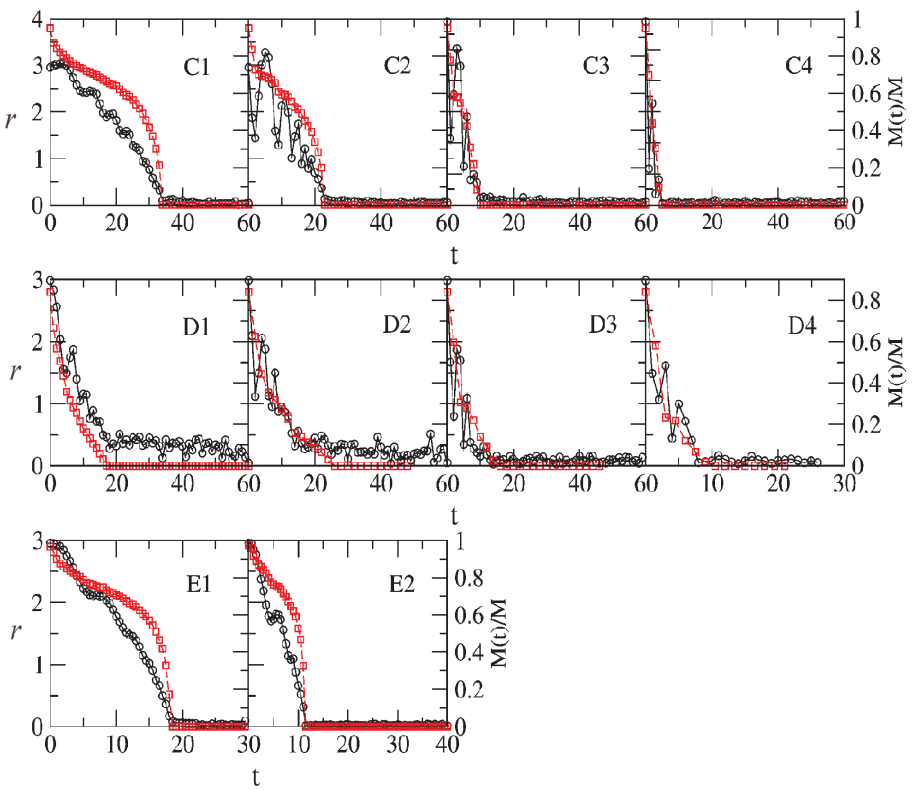

Fig. 5 Orbit and mass decay of satellite for Model C, D and E. The X-axis of these panels is time in unit of 10^8 years. The Y-axis plotted at the left hand is the orbital radius of the simulated satellite, and, at the right hand, is the mass fraction of the satellite. The solid lines with circles show the orbit evolution. The dashed lines with squares show the mass decay. Because the satellites are not rigid, tidal effects play a role in these models.

In Chandrasekhar's dynamical friction formula, the predicted merging time scale is proportional to $M_{\rm sat}^{-1}$. In tidal stripping this scaling is expected to change. We examine such change using our simulations of Models C1, E1 and E2. In all these simulations both the host and the satellite have a Hernquist profile, and the orbital circularity are all set to be 1, the only difference is of the satellite mass (See Table 1). Although the samples are not large there is a

clear correlation between the merging time scale and the initial mass of the satellite (Fig. 9). A power-law fit to the correlation gives

$$\tau_{\rm merg} \propto (\frac{m_{\rm sat}}{m_{\rm host}})^{-0.89}, \tag{6}$$

with a power index only slightly different from -1.

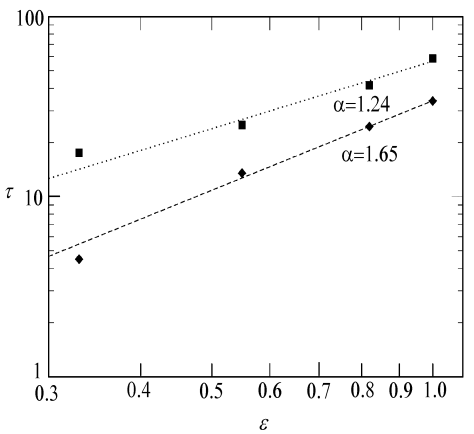

Fig. 6 Relation between the merging time scale and the orbital circularity of satellites for Model C series compared with Model B1-B4. Squares are for Model B and diamonds for Model C. The dot and dashed lines are best fits for the data points. The relation can be fitted by a power law and the power index is indicated in the figure. The different slope comes from the mass distribution of the satellite and tidal stripping.

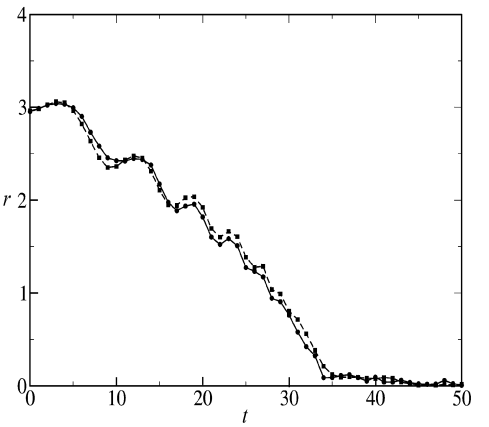

Fig. 7 Orbital decay of the satellites in Model C1 and F1. The full line with dots refers to the satellite in C1, and the dashed line with squares, to Model F1. The numerical resolution of F1 is 10 times higher than that of C1, but the features of orbital decay of these two simulations are almost the same. Numerical effects do not play a role in shortening the merging time of non-rigid satellites.

In addition to merging time we also explore other issues associated with tidal effects from our merging simulations. The structural properties of the satellites and the mixing of the stripped material in the host halos are investigated with models of series C, D and E. In Fig. 5, the squares connected by dashed lines show the mass decay of the merging satellites. With mass stripped, the structure of the satellite is expected to change. Hayashi et al. (2002) presented their simulation results on the structure evolution of NFW sub-halos subjected to tidal stripping by host halos. They proposed a fitting formula to describe the density profile of the stripped sub-halos,

$$\rho(r) = \frac{f_t}{1 + (r/r_{\rm te})^3} \rho_{\rm NFW}(r), \tag{7}$$

where f_t is a dimensionless measure of the reduction in central density, and $r_{\rm te}$ is an 'effective' tidal radius. Following their suggestion we fit the density profiles of our stripped satellites with a similar function,

$$\rho(r) = \frac{f_t}{1 + (r/r_{\rm te})^3} \rho_{\rm origin}(r). \tag{8}$$

Here, we replace $\rho_{\rm NFW}(r)$ by $\rho_{\rm origin}(r)$, the original density profile of the satellite. As one can see from Fig. 10, this fitting formula gives a remarkably good description of our data.

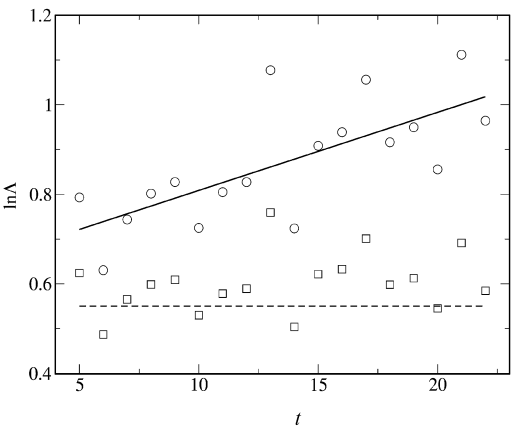

Fig. 8 Morphology evolution due to tidal stripping is ruled out as the reason of speeding up the merger. The circles denote the Coulomb logarithm of the satellite in Model C1. The value of $\ln\Lambda$ is calculated with Equation 7, for the satellites at snapshot time from $t = 5$ to $t = 22$. The X-axis is time, in units of 10^8 Gyr. The squares denote the value of $\frac{m_{\rm sat}(t)}{m_{\rm sat}(0)}\ln\Lambda$. There is no obvious increasing trend for this quantity. The dashed line shows the original value of $\ln\Lambda$ of the satellite.

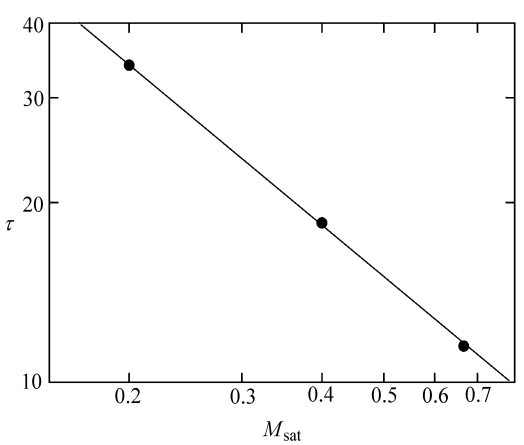

Fig. 9 Dependence of merging time scale on the mass of the satellite. The mass is in units of $10^{11}M_\odot$. The relation is fitted by $\tau \propto M_{\rm sat}^{-\alpha}$, $\alpha = 0.89$. The slope is different from 1 due to the tidal stripping.

An important quantity describing tidal stripping is the tidal radius. In our simulations, we find that the tidal truncation is not sharp, and the density goes only slowly to zero in the outer region. Because of this, we define a tidal radius at which the density of the bound part is reduced by a factor of 2. This definition has a more physical meaning: the tidal radius so

defined is closely correlated with the local density of the host at the location of the satellite. As shown in Fig. 11, this correlation follows closely the relation

$$m(t)/l_t^3 = M(r)/r^3, \tag{9}$$

where $m(t)$ is mass of the satellite at time t, $M(r)$ the mass profile of the host (e.g. Weinberg 1994), l_t the tidal radius and r the orbit radius of the satellite at time t.

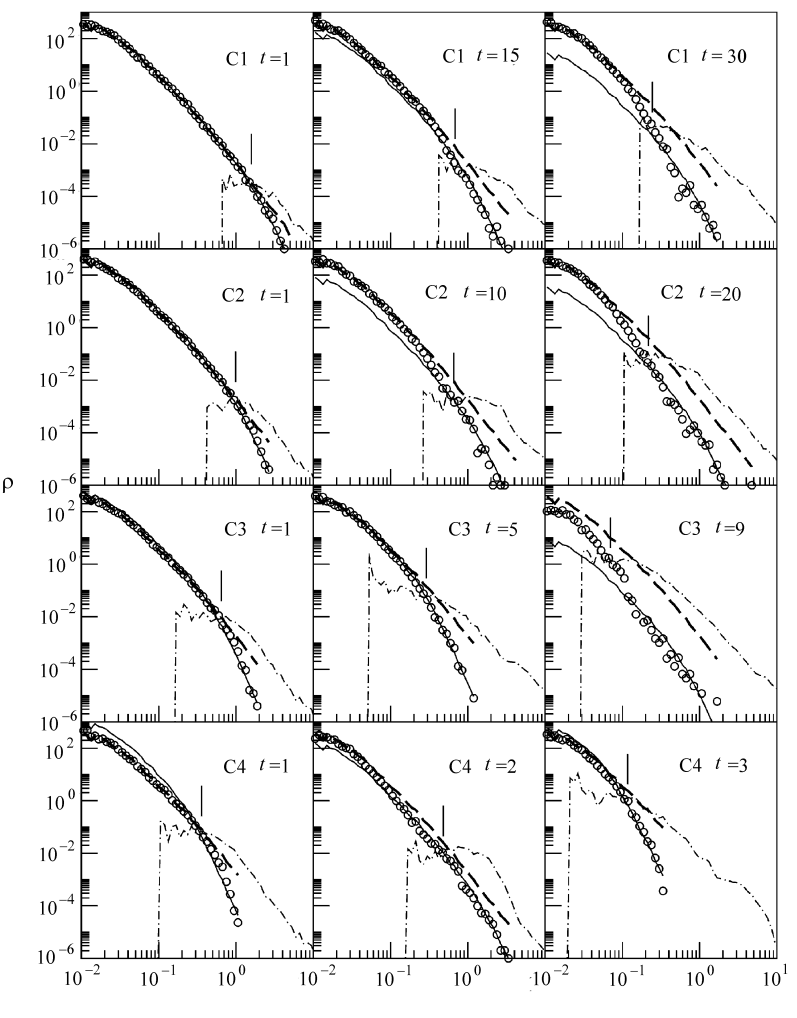

Fig. 10 Evolution of density profile of satellites. The X-axis represents radius and the Y-axis represents density. Each row is plotted for one model, and the three panels are taken at different time, when the merger happens at the very beginning, at the halfway time, and just before the satellite is disrupted. In each panel, the circles denote the density distribution of the bound satellite. The dashed line shows the original profile. The solid line curves the best fitting with Equation 10. The dashed-dot line shows the distribution of the stripped mass. The short vertical line points to the tidal radius as we defined.

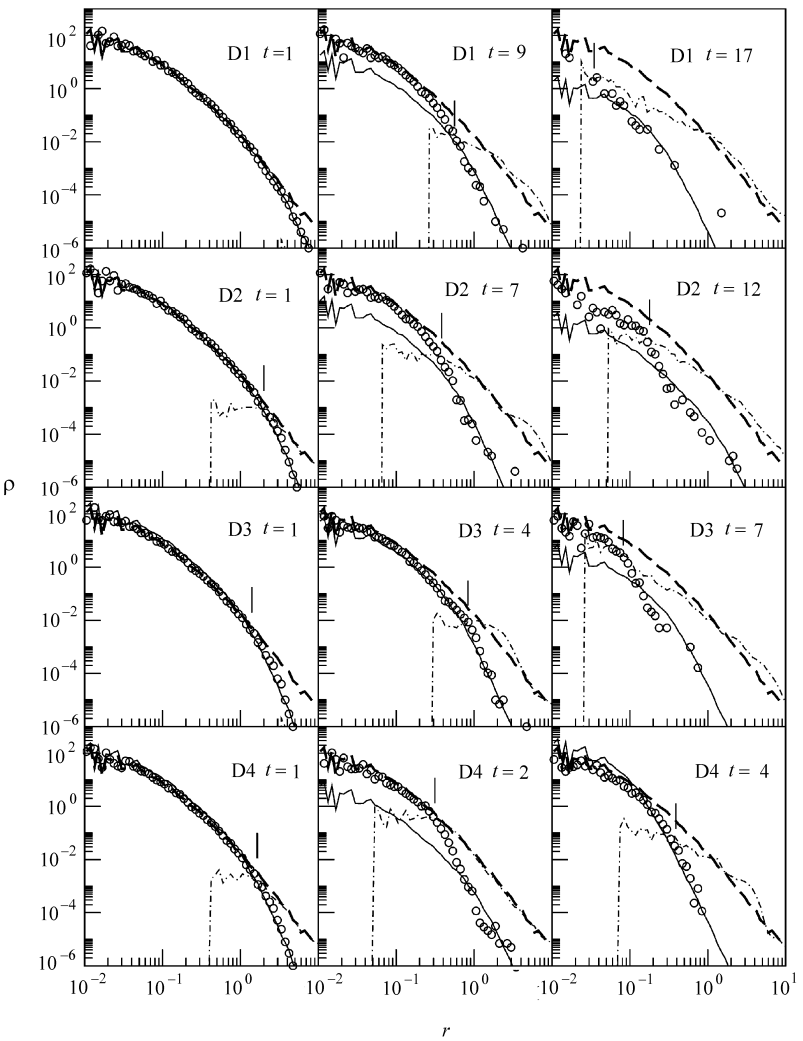

Fig. 10 Continued.

In a model considered by Maller & Dekel (2002), it is assumed that as material is stripped from a satellite the stripped material is added to the halo, retaining its angular momentum. In this case the angular momentum of a stripped particle should be equal to the orbital angular momentum of the satellite at the time when it is stripped. We can examine whether or not this assumption is correct by plotting the angular-momentum distribution of the particles that are stripped over the time between two successive snapshots. The distribution appears to show double peaks, one located at a value slightly lower than the current orbital angular momentum of the bound satellite, and the other, at a significantly higher value (See Figure 12). The ratio between the average specific angular momentum of the stripped particles and that of the

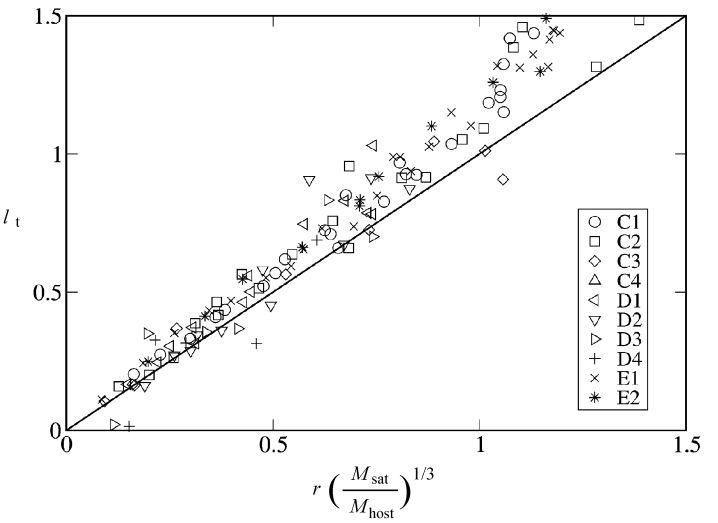

Fig. 11 Correlation between the tidal radius and the distance from the host center to the satellite. Here r is the orbital radius of the satellite, $M_{\rm sat}$ the mass of the bound satellite, $M_{\rm host}$ the mass of the host halo within r, and l_t the tidal radius as we defined.

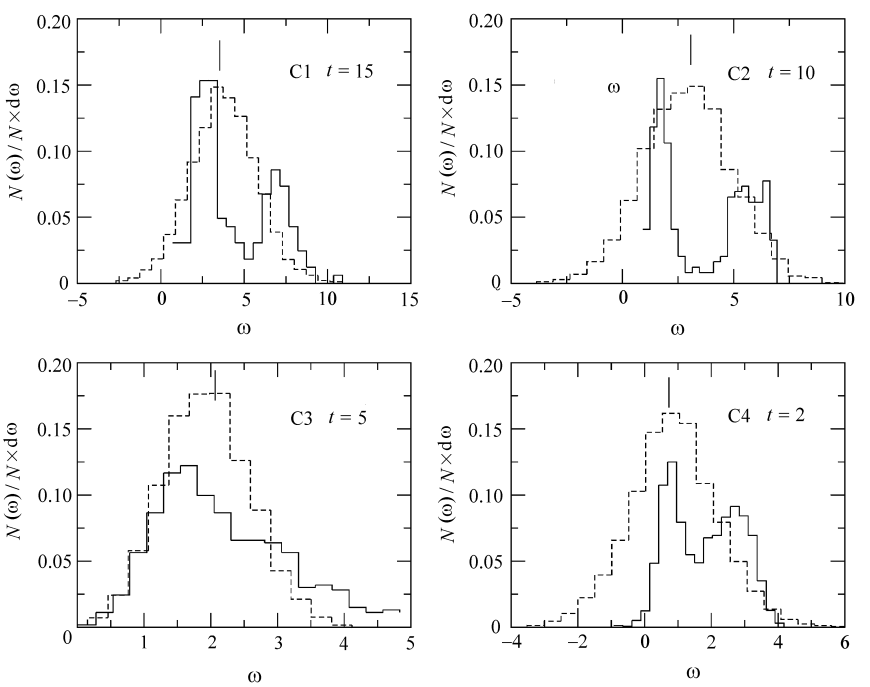

Fig. 12 Angular momentum distribution of stripped and bound particles for model C series at given time during merging. Time in units of 10^8 years is shown in upper right corner of each frame. Solid symbols for stripped particles, dashed ones for bound particles. The x-axis is specific angular momentum. The vertical dashes point is the current specific orbital angular momentum of the bound satellite.

retained particles is about 1.2, meaning that the satellite loses orbital angular momentum due to stripping. This is the reason why the non-rigid satellites in Model C sink into the halo center faster than rigid ones in Model B. Identifying the particles contributing to these two peaks, we find that the lower angular momentum particles are stripped from the side facing the center of the host, while the higher angular momentum peak is dominated by particles stripped from the back side of the satellite (see Fig. 13). The low angular momentum particles are sinking towards the host center, while the high angular momentum particles form a tail-like structure spiraling at larger radii.

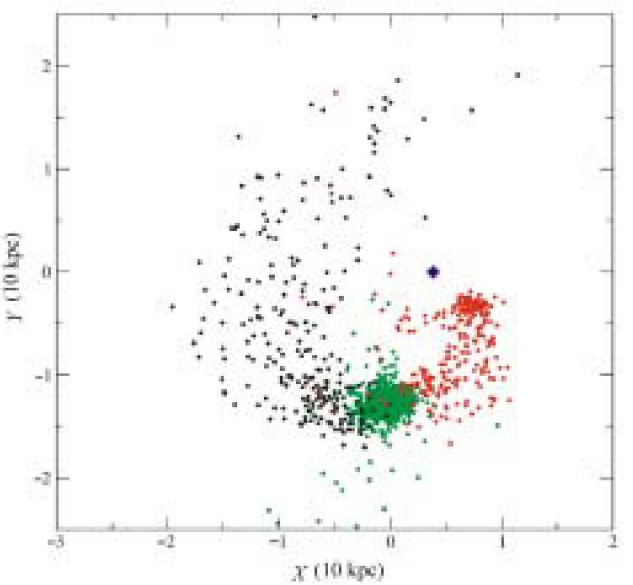

Fig. 13 This snapshot is taken at $t = 30$ for model C1. The red spots show the escaping particles with low angular momentum at this time, and the black spots show the escaping particles with high angular momentum. The green points are the bound particles. The blue diamond marks the center of the host.

5 CONCLUSIONS AND DISCUSSION

In this paper we present results of controlled numerical experiments of minor mergers, focusing our attention on merging time and tidal effects. We confirm the power-law relation between the merging time scale and the circularity of satellites. We find the power index depends on the mass distribution of the host halo. For non-rigid satellites, the merging time scale also depends on the initial mass of the satellite as a power-law. An interesting point is that a satellite which can be stripped falls into the center of the host faster than a rigid one. Using White's (1976) model on the Coulomb logarithm, we can rule out structural evolution of the satellite as the cause of this phenomenon. We also find that tidal interaction can launch a significant amount of high angular momentum material from the satellite, accelerating the orbital decay of the satellite.

We also studied the structural properties of the satellites during the merger process. We define a tidal radius which has a close correlation with the location of the satellite in its host and the satellite/host mass ratio. This result is useful in determining the size and the mass of merging satellites.

Acknowledgements We thank Hou-Jun Mo and Yi-Peng Jing for instructive discussions. We thank Simon White for helpful suggestion. This work was carried out partly by using the Yin-He Super-computer, based at the Institute of Applied Physics and Computational Mathematics, Beijing, and the Dawning 2000II Super-computer based at the Computer Network Information Center, Chinese Academy of Sciences.

References

Binney J., Tremaine S., 1987, Galactic Dynamics, Princeton: Princeton University Press
Bontekoe T. R., van Albada T. S., 1987, MNRAS, 224, 349
van den Bosch F. C., Lewis G. F., Lake G., Stadel J., 1999, ApJ, 515, 50
Chandrasekhar S., 1943, ApJ, 97, 255
Hayashi E., Navarro J. F., Taylor J. E., 2003, ApJ, 584, 541
Hernquist L., 1990, ApJ, 356, 359
van Kampen E., 2000, preprint [astro-ph/0002027]
Lacey C., Cole S., 1993, MNRAS, 262, 627
Maller A. H., Dekel A., 2002, MNRAS, 335, 487
Navarro J. F., Frenk C. S., White S. D. M., 1996, ApJ, 462, 563
Sensui T., Funato Y., Makino J., 2002, PASJ, 51, 1
Springel V., Yoshida N., White S. D. M., 2001, New Astron., 6, 79
Tormen G., Diaferio A., Syer D., 1998, MNRAS, 299, 728
Velázquez H., White S. D. M., 1999, 304, 254
Weinberg M. D., 1994, AJ, 108, 1398
White S. D. M., 1976, MNRAS, 174, 467